INSTITUTE OF EXPERIMENTAL PHYSICS
SLOVAK ACADEMY OF SCIENCES

THE 15th SMALL TRIANGLE MEETING

on Theoretical Physics

October 27–30, 2013

Stará Lesná

The 15th Small Triangle Meeting on theoretical physics was supported by the Project of Structural funds of EU-Centrum Excellence: Cooperative Phenomena and Phase Transitions in Nanosystem with perspective utilization in Technics and Biomedicine No: 26220120021 and Centre of Excellence Nanofluids of Slovak Academy of Sciences.

Published by the Institute of Experimental Physics, Watsonova 47, 040 01 Košice, Slovakia

Edited by J. Buša, M. Hnatič, and P. Kopčanský

Printed in the Institute of Experimental Physics, 2014

ISBN 978-80-8143-141-8

15th Small Triangle Meeting — Stará Lesná, October 27–30, 2013

Electroconvection in a Nematic Liquid Crystal under Superposed AC and DC Electric Voltages

N. Éber[1], P. Salamon[1], B. Fekete[1], T. Tóth-Katona[1], R. Karapinar[2,1], M. Sacks[3,1], Á. Buka[1]

[1] *Institute for Solid State Physics and Optics, Wigner Research Centre for Physics of HAS, H-1525 Budapest, P.O.B.49, Hungary*
[2] *100. Yil University,Department of Physics, 650580 Van, Turkey*
[3] *Allegheny College, 520 N. Main Street, Meadville, PA 16335, USA*

Abstract

The behaviour of an electric field induced pattern forming instability, the electroconvection in a nematic liquid crystal, was studied under the influence of superposed dc and ac electric voltages. The onset parameters (threshold voltages and critical wave numbers) were determined. It was found that the superposition of voltages inhibits the pattern forming mechanism; therefore the patternless region extends to much higher voltages than the individual ac or dc thresholds. A dc bias induced reduction of the electrical conductivity and a shift of the crossover frequency from the conductive to dielectric electroconvection regimes were also detected.

Nematic liquid crystals are anisotropic fluids with an orientational order characterized by the preferred direction of their molecules, the director $\mathbf{n}(\mathbf{r})$, which can be (re)oriented by an electric field $\mathbf{E}$ [1]. In most experiments and applications thin (5-20 μm) liquid crystal films are sandwiched between transparent electrodes and a uniform quiescent state is ensured by proper surface aligning techniques. Upon applying an electric voltage V exceeding some critical value V_c, director distortions may occur [1]. Display applications require this distortion be uniform in the cell plane; however, under certain conditions complex spatio-temporal structures, patterns, can also be induced. Here we will deal exclusively with a particular dissipative pattern forming phenomenon, the standard electroconvection (EC) [2]. The resulting patterns correspond to a spatially periodic system of convection rolls of a wave vector $\mathbf{q}$, which appear as dark and bright stripes in a polarizing microscope.

Standard EC is mostly observed in planar nematics having a negative dielectric anisotropy $\varepsilon_a < 0$ and a positive electrical conductivity anisotropy $\sigma_a > 0$. EC can be induced by dc (V_{dc}) as well as by ac (V_{ac}) voltages. In the latter case V_{ac} corresponds to the rms value of the driving sinusoidal voltage of frequency f. Its driving feedback mechanism was invented by Carr and Helfrich [2]: a spatial director fluctuation $\mathbf{n}(\mathbf{r})$ leads to space charge separation $\varrho_e(\mathbf{r})$ due to σ_a; the Coulomb force induces a flow $\mathbf{v}(\mathbf{r})$ forming vortices due to the constraining

surfaces; the flow exerts a destabilizing torque on the director. For $V < V_c$ the fluctuations decay; however, they grow to a macroscopic pattern for $V > V_c$.

By now standard EC has quite well been understood. Its precise continuum theoretical description is known as the standard model (SM) of EC [3]. Recently this has been further improved by including contributions from flexoelectricity (the extended SM [4, 5]). They are composed of equations for the director relaxation, for the material flow and for the space charge (or the electric potential) distribution with the assumption of ohmic conductivity of the liquid crystal. These models provide the frequency dependent thresholds $V_c(f)$, the critical wave vectors $\mathbf{q}_c(f)$ and the spatio-temporal dependence of the director $\mathbf{n}(\mathbf{r}, t)$ at the onset, in good accordance with experiments. Inspection of the equations shows that they have solutions with 3 different time symmetries. One is for the dc driving (we will refer to it as the *dc-mode*): in this case $\mathbf{n}(\mathbf{r})$, $\mathbf{v}(\mathbf{r})$ and $\varrho_e(\mathbf{r})$ are time independent. The other two occurs at ac driving: in the *conductive mode* the director and the velocity is almost stationary (at least for frequencies above the inverse director relaxation time [6]), i.e. the time average of the director tilt over the driving period is nonzero ($\langle n_z(t)\rangle \neq 0$) while space charges oscillate with f; in the dielectric mode, on the contrary, $\varrho_e(\mathbf{r})$ is stationary while $\mathbf{n}(\mathbf{r})$, $\mathbf{v}(\mathbf{r})$ oscillate with f (i.e. $\langle n_z(t)\rangle = 0$). The two ac modes have different pattern morphologies (different $\mathbf{q}$) and the shapes of the $V_c(f)$ curves also differ [2]; therefore, at a given f that pattern occurs actually, which has a lower threshold voltage.

As standard EC may occur at pure dc as well as at pure ac excitation, one expects it to arise at a combined driving (superposed ac and dc voltages) too. This field is, however, experimentally almost unexplored. So far we are aware of only one report about the effect of combined (ac+dc) driving on electroconvection, where in the nematic 5CB (4-pentyl-4'-cyanobiphenyl) changes in the threshold voltages and also appearance of new pattern morphologies were detected [7]. In that compound, however, $\varepsilon_a > 0$ and $\sigma_a > 0$; for this combination of parameters the extended SM does not predict any instability. Therefore the observed patterns are due to a still unidentified mechanism and are categorized as nonstandard EC.

The consequences of the combined driving in standard EC are non-trivial also from theoretical point of view; the solution may not be obtained as a simple superposition of the three modes of different time symmetries mentioned above. This complexity of the temporal behaviour deserves a special interest and served as our main motivation to extend our EC studies to the case of combined driving.

Our experiments have been carried out on $d = 10.8$ μm thick, planarly aligned sandwich cells (E.H.C. Co., Japan) of the room temperature nematic mixture Phase 5 (Merck), which has often been used in former EC studies [8, 9, 6]. The sample was placed into a temperature controlled compartment ($T = 30 \pm 0.05$ °C) under a polarizing microscope.

A driving voltage of $V(t) = V_{dc} + \sqrt{2}V_{ac}sin(\omega t)$ with arbitrary V_{dc}/V_{ac} ratio was applied to the cell from a function generator through a high voltage amplifier. A digital oscilloscope was used to record the temporal evolution of the applied voltage and the current flowing through the cell. The voltage-induced patterns were observed and recorded using the shadowgraph technique at white light illumination with a digital camera attached to the microscope.

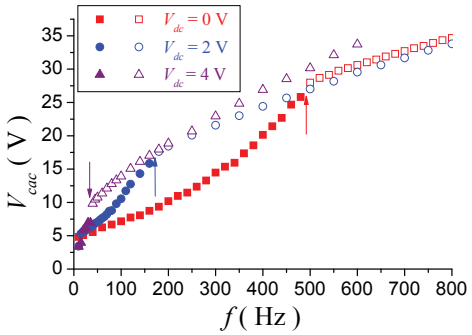

Figure 1: The measured frequency dependence of the ac threshold voltage V_{cac} of EC in a Phase 5 sample at various dc bias voltages V_{dc}. Solid symbols correspond to the conductive regime, open symbols to the dielectric one. The arrows indicate the frequency of crossover between the two morphologies.

At pure dc driving Phase 5 exhibits the dc mode of EC for voltages $V > V_{cdc0} \approx 5 - 6$ V. Under pure sinusoidal ac driving one observes a frequency dependent threshold voltage $V_{cac0}(f)$, which is depicted in Fig. 1. Depending on f two distinct EC regimes can be identified: in the low f range (conductive regime) $V_{cac0}(f)$ increases strongly with f, then at the crossover frequency f_c a transition to the dielectric regime occurs indicated by the reduction of the slope. The two regimes are characterized by different pattern morphologies (different q_c values). This behaviour agrees well with previous observations [8, 9, 6]. We note that both V_{cac0} and f_c depend strongly on the electrical conductivity.

Figure 1 also presents the frequency dependence of the ac threshold voltages $V_{cac}(f)$ for two different dc bias voltages ($V_{dc} = 2$ V and 4 V). The curves obtained in the presence of a dc bias voltage are qualitatively similar to those at pure ac, only the crossover frequency (indicated by arrows in Fig. 1) is substantially reduced. At a fixed f this is typically equivalent to the increase of the pattern threshold upon increasing the dc bias.

Note that no curves for higher dc bias voltages could be shown as for $V_{dc} > V_{cdc0}$ the dc voltage already induces a pattern by itself.

In the following we focus on the behaviour at fixed frequencies looking for the critical combination of ac and dc voltages where patterns appear (or disappear). In order to allow comparison the same strategy was followed for all tested frequencies: first the ac voltage was fixed, then the dc bias voltage was increased to find the morphological transition(s).

Let us start with the scenario at low frequency ($f = 80$ Hz). Figure 2(a) shows the morphological phase diagram in the $V_{ac} - V_{dc}$ plane. Data points correspond to the boundaries $V_{cdc}(V_{cac})$ of the patternless region, which is composed of three branches. 1) The upper (dc) branch starts at $V_{dc} = V_{cdc0}$ and V_{cdc} of the dc pattern mode is slightly increasing with the added ac voltage. The scattering in the data indicates the uncertainties in threshold determination. Figures 3(a) and 3(b) exhibit the patterns observed slightly above onset for low and high V_{ac},

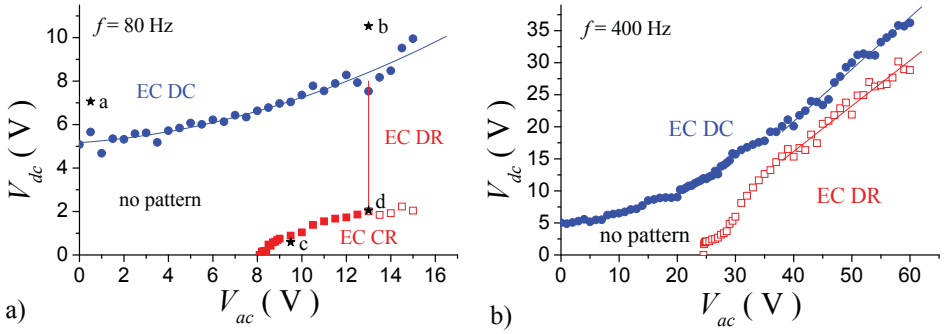

Figure 2: Morphological phase diagram of a Phase 5 sample at a) $f = 80$ Hz and b) at $f = 400$ Hz. The lines are guides for the eyes. The stars mark the points where the snapshots shown in Fig. 3 were taken. Note that the conductivity of the tested sample was lower than that of the one used in Fig. 1.

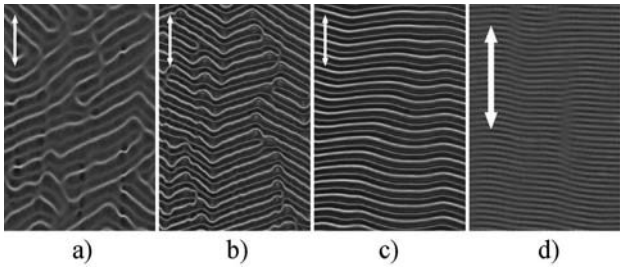

Figure 3: Typical EC pattern morphologies of a Phase 5 sample at $f = 80$ Hz: a) oblique rolls of dc mode at $V_{ac} = 0.5$ V, $V_{dc} = 7.06$ V; b) oblique rolls at $V_{ac} = 13.0$ V, $V_{dc} = 10.53$ V; c)conductive rolls at $V_{ac} = 9.5$ V, $V_{dc} = 0.59$ V; d) dielectric rolls at $V_{ac} = 13.0$ V, $V_{dc} = 2.05$ V (note the change in the magnification). The double arrows show the direction of the initial director; their length corresponds to 50 μm.

respectively. They are oblique rolls with the dimensionless wave number $q^* = \frac{2d}{\lambda} \approx 1$ (slightly increasing with V_{ac}). Here λ is the wavelength of the pattern. 2) The lower (ac) branch, starting at $V_{ac} = V_{cac0} \approx 8$ V, corresponds to the ac conductive regime. Note, that this threshold voltage is higher than that deducible from Fig. 1; the deviation is due to the different electrical conductivity of the samples. A typical pattern is shown in Fig. 3(c); q^* is similar to that on the upper branch, but the angle of obliqueness is close to zero. Moving along this branch for higher V_{ac} (which means the increase of V_{dc} too) a morphological transition is found at $V_{ac} \approx 13$ V to the ac dielectric regime, which is indicated by a jump in the wavenumber of the pattern to $q^* \approx 6$ (see Fig. 3(d)). 3) The upper (dc) and the lower (ac) branches run nearly parallel for $10 \lessapprox V_{ac} \lessapprox 13$ V, thus opening a 'channel' for the patternless region to extend to voltages exceeding substantially either V_{cac0} or V_{cdc0}. This channel is closed by the third branch, a nearly vertical

line at $V_{ac3} \approx 13$ V. For $V_{ac} > V_{ac3}$ pattern exists for any dc voltages. V_{ac3} coincides with the voltage inducing the transition from conductive to dielectric regime. We note that this is, however, accidental for the selected frequency. For lower f the morphological phase diagrams are similar to that in Fig. 2(a), just the lower and the third branches are shifted toward lower ac voltages; therefore the closure of the channel occurs still in the conductive regime.

Increasing the frequency the scenario gradually changes: along the lower branch one always sees normal rolls of the dielectric regime; their onset requires higher ac voltages and the patternless channel extends to higher V_{ac} and V_{dc} values. Finally, at $f = 400$ Hz the upper (dc) and the lower (ac) branches run almost parallel in a wide voltage range as seen in Fig. 2(b) and do not join up to the highest available voltage applied (limited to ± 200 V peak by the high voltage amplifier). As a consequence, there are V_{ac}, V_{dc} combinations where no pattern occurs, even though each voltage is several times higher than the thresholds V_{cac0} and V_{cdc0} belonging to the pure ac or pure dc driving, respectively. This shows that superposing ac and dc voltages suppresses their ability to induce pattern formation.

The electrical conductivity of liquid crystals is mostly originating from the ions present in them. Therefore one expects that applying dc bias voltages may alter the number and distribution of the charge carriers and thus the conductivity. Our electric current measurements have confirmed this expectation. The parallel resistance R_p of the sample gradually increases with increasing V_{dc}, reaching $4-5$ times higher values at large dc voltages than at $V_{dc} = 0$. We note that upon removing the dc bias R_p relaxes partially on a time scale of minutes. Full recovery of the initial resistance, if it occurs at all, may require several days.

It is known from the SM that the ac threshold voltages depend strongly on the conductivity of the sample in the conductive regime, while they are less sensitive in the dielectric regime. Therefore the dc bias induced decrease of the conductivity can explain the reduction of the frequency f_c of the crossover from conductive to dielectric patterns shown in Fig. 1 as well as the voltage induced crossover between the same regimes along the lower branch in Fig. 2(a).

In principle the SM is capable to provide the $V_{cdc}(V_{cac})$ curves for EC at combined driving too. Preliminary calculations at a constant conductivity indicated [10], on the one hand, that the dc threshold voltage of the dc mode (upper branch) has to increase upon superposing an ac voltage, which is in agreement with our observations. On the other hand, the ac threshold voltages of the ac modes (independently whether conductive or dielectric) should decrease upon adding a dc bias voltage, which clearly disagrees with the results shown in Fig. 2.

Summarizing, we have proven that EC patterns with different morphologies occur also at superposed ac and dc voltages. Surprisingly the superposition hinders the pattern forming mechanisms; the combined threshold voltages may be substantially higher than those at pure dc or ac driving which does not match with the theoretical expectations. Possible reasons for this discrepancy may be the simplifications used in the SM; namely, it cannot handle a voltage dependent conductivity and cannot account for the electric field gradients occurring near the

electrodes in the presence of dc voltages. A detailed analysis of these effects means a great theoretical challenge for the future.

Financial support by the Hungarian Research Fund OTKA K81250 is gratefully acknowledged. N. É and T. T.-K. are thankful for the hospitality provided in the framework of the HAS-SAS bilateral mobility grant SNK71/2013. M.S. thanks D. Statman and the National Science Foundation International Research Experience for Students (NSF-IRES) grant for their support. Fruitful discussions with W. Pesch and A. Krekhov are highly appreciated.

References

[1] L.M. Blinov and V.G. Chigrinov, *Electrooptic Effects in Liquid Crystal Materials* (Springer, New York, 1996).

[2] L. Kramer, and W. Pesch, In eds. Á. Buka, and L. Kramer, *Pattern Formation in Liquid Crystals.* pp. 221-256. (Springer-Verlag, New York, 1996).

[3] E. Bodenschatz, W. Zimmermann, and L. Kramer, *J. Phys. (France)* **49**(11), 1875–1899, (1988).

[4] A. Krekhov, W. Pesch, N. Éber, T. Tóth-Katona, and Á. Buka, *Phys. Rev. E* **77**(2), 021705/1–11, (2008).

[5] A. Krekhov, W. Pesch, and Á. Buka, *Phys. Rev. E* **83**(5), 051706/1–13, (2011).

[6] N. Éber, L. O. Palomares, P. Salamon, A. Krekhov and Á. Buka, *Phys. Rev. E* **86**, 021702/1–9, (2012).

[7] L. E. Aguirre, E. Anoardo, N. Éber and Á. Buka, *Phys. Rev. E* **85**, 041703/1–9, (2012).

[8] M. Treiber, N. Éber, Á. Buka, and L. Kramer, *J. Physique II*, **7**, 649-661 (1997).

[9] T. Tóth-Katona, N. Éber, Á. Buka, and A. Krekhov, *Phys. Rev. E* **78**(3), 036306/1–12, (2008).

[10] W. Pesch, and A. Krekhov, private communication.